Development of Geothermal Reservoir Simulator Dealing with Mineral Reactions

Daichi Tanabu and Masanori Kurihara

Waseda University

Keywords

Reservoir simulator, Chemical reaction, Mineral dissolution

ABSTRACT

Most of general geothermal simulators assume the pure water as a geothermal reservoir fluid. However, since it actually contains chemical species, the geothermal reservoir performances predicted by these general simulators may be different from actual ones. Therefore, in this study, we tried to develop the geothermal reservoir simulator that can take the effects of chemical species in water phase and chemical reactions between fluid and reservoir rock into consideration.

The simulator developed in this study can deal with not only the water/steam flow and associated temperature change but also the chemical reactions such as dissolution of rock minerals and precipitation of solutes. That is, the chemical species concentrations are simulated in accordance with the equations expressing the kinetic reactions, convection and dispersion of chemical species. The effects of chemical species concentration such as elevation of boiling point, heat of reaction and changes in porosity/permeability are also considered. To verify the performances of this simulator, the results predicted by this simulator assuming no chemical reactions are compared with those by the commercial thermal simulator, followed by the validation of the accurate calculation for the influences of chemical species with analytical solutions.

Finally, we conducted the case studies to examine how the chemical composition and/or temperature of recharge water affected geothermal reservoir behavior. Through these studies it was revealed that (1) the injection of the water with low salt concentration induced the dissolution of rock minerals while that of the water with excessive ion concentration resulted in precipitation of solutes near the injection well, (2) the change in reservoir temperature caused the mineral dissolution/precipitation due to the alteration of chemical equilibrium and (3) the magnitude of porosity and permeability changes associated with dissolution/precipitation of minerals might not be large.

1. Introduction

In the operation of geothermal power generation, it is important to consider the chemical components contained in the geothermal fluid. It is anticipated that these chemical components may be deposited in surface facilities or initiate chemical reactions in a reservoir to change their properties. However, because most of general geothermal simulators assume the pure water as a geothermal reservoir fluid, the geothermal reservoir performances predicted by these general simulators may be different from actual ones. Therefore, in this study, we tried to develop the geothermal reservoir simulator that can take the effects of chemical species in water phase and chemical reactions between fluid and reservoir rock into consideration.

2. Construction of Reservoir Simulator

2.1 Governing Equations

In a geothermal simulator, two equations for water/steam mass balance and for energy balance are generally adopted as governing equations. In contrast, in this study, the number of governing equations is increased according to the number of chemical species. The governing equations for the component "c" and the energy balance equation are shown below. Equation (1) is the material balance equation for water component, taking account of the water in water phase and steam in gas phase. Equation (2) is the material balance equation for ionic components, which exist only in the water phase. Equation (3) expresses the material balance for solid (mineral) components, which is stagnant in a reservoir. The energy balance is given by Equation (4).

$$\frac{\partial}{\partial x}\left(\frac{kk_{rw}}{\mu_w}\frac{\partial \Phi_w}{\partial x}\rho_w w_w^c\right)+\frac{\partial}{\partial x}\left(\frac{kk_{rg}}{\mu_g}\frac{\partial \Phi_g}{\partial x}\rho_g w_g^c\right) + r_{reaction}^c+\tilde{q}_w\rho_w{}'w_w^{c\prime}+\tilde{q}_g\rho_g{}'w_g^{c\prime}=\frac{\partial}{\partial t}\left\{\left(\rho_w S_w w_w^c+\rho_g S_g w_g^c\right)\phi\right\} \tag{1}$$

$$\frac{\partial}{\partial x}\left(\frac{kk_{rw}}{\mu_w}\frac{\partial \Phi_w}{\partial x}\rho_w w_w^c\right)+r_{reaction}^c+\tilde{q}_w\rho_w{}'w_w^{c\prime}=\frac{\partial}{\partial t}\left(\rho_w S_w w_w^c\phi\right) \tag{2}$$

$$r_{reaction}^c=\frac{\partial}{\partial t}\left\{\rho_s w_s^c(1-\phi)\right\} \tag{3}$$

$$\frac{\partial}{\partial x}\left(\frac{kk_{rw}}{\mu_w}\frac{\partial \Phi_w}{\partial x}\rho_w H_w\right)+\frac{\partial}{\partial x}\left(\frac{kk_{rg}}{\mu_g}\frac{\partial \Phi_g}{\partial x}\rho_g H_g\right)+\frac{\partial}{\partial x}\left(\lambda_{all}\frac{\partial T}{\partial x}\right) + r_{reactionheat}+\tilde{q}_w\rho_w{}'H_w{}'+\tilde{q}_g\rho_g{}'H_g{}' =\frac{\partial}{\partial t}\left\{\left(\rho_w S_w U_w+\rho_g S_g U_g\right)\phi+\rho_s U_s(1-\phi)\right\} \tag{4}$$

where

Φ_P : Potential of phase p [Pa]

k : Absolute permeability [m^2]

k_{rp} : Relative permeability to phase p [-]

μ_p : Viscosity of phase p [Pa·s]

ρ_p : Molar density of phase p [mol/m^3]

ρ_p' : Molar density of phase p of injection fluid [mol/m^3]

w_p^c : Mole fraction of component c in phase p [-]

$w_p^{c\prime}$: Mole fraction of component c in phase p of injection fluid [-]

$r_{reaction}^c$: Generation rate of component c per unit bulk volume [$mol/m^3/s$]

$\tilde{q}_p$: Injection/production rate of phase p per unit bulk volume [1/s]

S_p : Saturation of phase p [-]

ϕ : Porosity [-]

H_p : Molar enthalpy of phase p [J/mol]

U_p : Molar internal energy of phase p [J/mol]

T : Temperature [K]

λ_{all} : Total thermal conductivity [J/m/s/K]

$r_{reactionheat}$: Heat of reaction per unit bulk volume [$J/m^3/s$]

When the number of components is n_c, n_c+1 governing equations are established for n_c+1 primary unknowns. The simulator developed in this study solves Equations (1) through (4) simultaneously, discretizing these equations by finite difference method with implicit formula. The discretized equation system is then solved by Newton-Raphson method.

2.2 Chemical Reactions

In this study, we simply assumed the following three chemical reactions.

$$H_2O \leftrightarrow H^+ + OH^-$$

$$CaCO_3 + H^+ \leftrightarrow Ca^{2+} + HCO_3^-$$

$$HCO_3^- \leftrightarrow H^+ + CO_3^{2-}$$

Therefore, in this study, the simulator was designed so that it could deal with seven chemical species of H_2O, H^+, OH^-, $CaCO_3$, Ca^{2+}, HCO_3^- and CO_3^{2-}.

2.2.1 Chemical equilibrium constant

The chemical equilibrium constant is the activity product when the chemical reaction reaches equilibrium. For example, in the case of the chemical reaction of "$H_2O \leftrightarrow H^+ + OH^-$", the activity product is expressed by the following equation.

$$\theta = \frac{C_{H^+} C_{OH^-}}{C_{H_2O}}, \tag{5}$$

where

θ : Activity product [-]

C_c : Concentration of component c [mol/m^3]

The chemical equilibrium constant changes with each chemical reaction. The simulator calculates the generation rates per unit volume for each component associated with each chemical reaction by Equations (6) and (7). These equations are derived in accordance with the chemical kinetics, assuming the difference between the chemical equilibrium constant and the activity product as a driving force. Note that Equation (6) is applied to the reactions within the water phase (ionization), while Equation (7) is used for the reaction between the water phase and the solid phase (mineral dissolution/precipitation).

$$r^c_{reaction} = kC_{\min}\left(1 - \frac{\theta}{K_{eq}}\right)\phi S_w \tag{6}$$

$$r^c_{reaction} = kC_{\min}\left(1 - \frac{\theta}{K_{eq}}\right)(1-\phi)V^c_s, \tag{7}$$

where

k : Reaction rate constant [1/s]

C_{min} : Concentration of the minimum component [mol/m^3]

K_{eq} : Chemical equilibrium constant [-]

V_s^c : Volume fraction of component c in solid phase [-]

2.2.2 Elevation of boiling point

The boiling point temperature rises when non-volatile solids dissolve in liquid. The elevation of boiling point is proportional to the concentration of the solutes. The example of the difference in boiling point temperature between pure solvent and solution containing dissolved solids is illustrated in Figure 1.

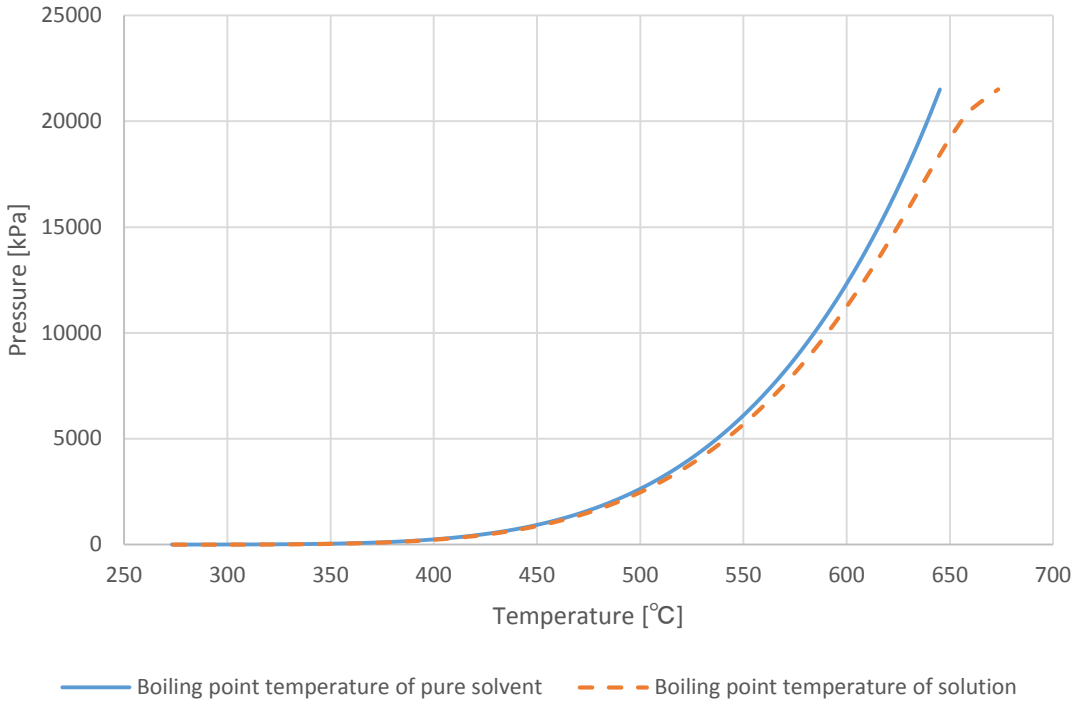

Figure 1: Example of elevation of boiling point

2.2.3 Heat of reaction

Thermal energy is released or absorbed along with the chemical reaction. The simulator takes this effect into consideration, by specifying the heat of reaction per mole for each chemical reaction.

2.2.4 Changes in porosity/permeability

Porosity and permeability change with the dissolution and/or precipitation of rock minerals, which is calculated as shown below.

First, the part of the rock mineral that can be reacted (dissolved) by chemical reactions is defined as A, while the other part (without reaction) is defined as B. The porosity of the rock is then calculated by solving Equation (8) because the volume of the part B never changes before and after the chemical reactions.

$$\left(1-\phi_{ref}\right)\left\{\frac{\left(\frac{w_s}{\rho_s}\right)^B}{\left(\frac{w_s}{\rho_s}\right)^A+\left(\frac{w_s}{\rho_s}\right)^B}\right\}=\left(1-\phi_{ref_{ini}}\right)\left\{\frac{\left(\frac{w_s}{\rho_s}\right)^B_{ini}}{\left(\frac{w_s}{\rho_s}\right)^A_{ini}+\left(\frac{w_s}{\rho_s}\right)^B_{ini}}\right\}, \tag{8}$$

where ϕ_{ref} denotes the reference porosity at the reference pressure. The true porosity can be obtained considering the influence of pressure by Equation (9).

$$\phi = \phi_{ref} \exp\left[C_p \left(P - P_{ref}\right)\right], \tag{9}$$

where C_p is the pore volume compressibility [1/Pa] and P_{ref} is the reference pressure [Pa]. Then the permeability is calculated based on the relationship between porosity and permeability expressed by Kozeny-Carman Equation.

3. Validation

To verify the performances of this simulator, the results predicted by this simulator assuming no chemical reactions were compared with those by the commercial thermal simulator, followed by the validation of the accurate calculation for the influences of chemical species with analytical solutions.

3.1 No Chemical Reaction Case

To validate the simulator developed in this study, we conducted the simulation using our simulator and the commercial thermal simulator "STARS" developed by Computer Modelling Group Ltd. (CMG) in accordance with the identical specifications. The results simulated by these two simulators were compared with each other.

3.1.1 Simulation specifications

As shown in Figure 2, the reservoir model used in this validation has the one-directional (10*1*1) grid system. The reservoir is initially filled with steam. Water is then injected into the grid 1 and the fluid is produced from grid 10. The simulation specifications are summarized in Table 1.

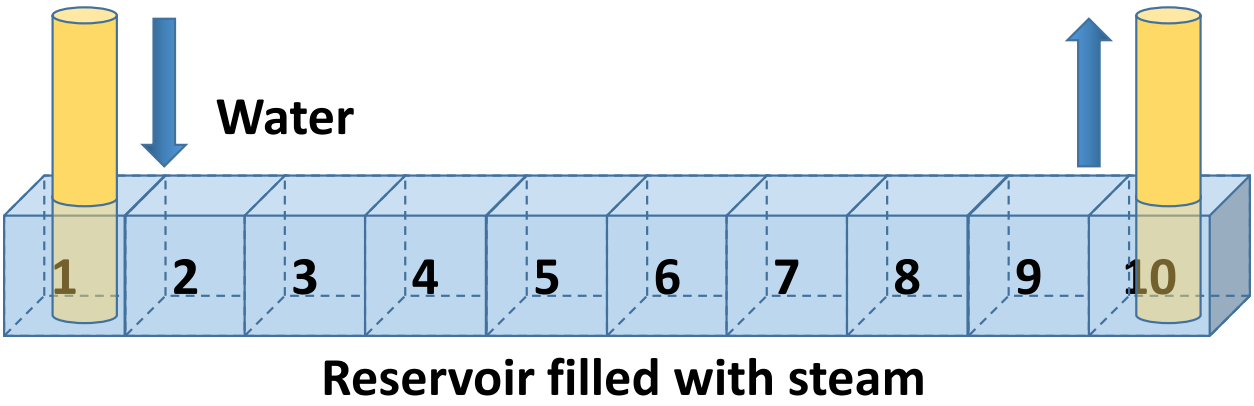

Figure 2: Reservoir model

Table 1: Simulation specifications

Item	Description
grid system nx, ny, nz	10, 1, 1
reservoir size [ft] x, y, z	1,000, 100, 100
initial pressure [psia]	1,500
initial temperature [°C]	350
initial water saturation [-]	0
absolute permeability [mD]	100
initial reference porosity ϕ_{ini} [-]	0.2
pore volume compressibility C_p [1/Pa]	1.450368394×10^{-9}
simulation time [day]	4,500

3.1.2 Results

The results of the above simulation such as pressure of grid 1, temperature of all the grids and water saturation of all the grids are depicted in Figure 3, Figure 4 and Figure 5, respectively. Note that the results by our simulator are captioned by “TANABU” and those by STARS are expressed by “STARS” in these figures.

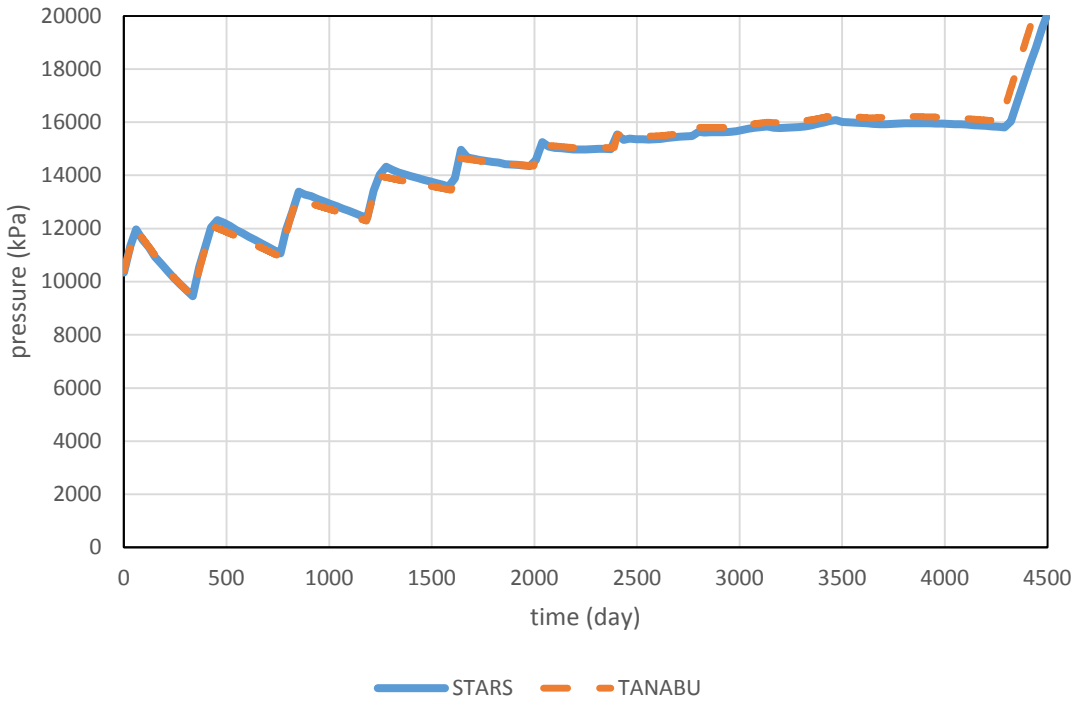

Figure 3: Time vs. pressure at grid 1 (injection well grid)

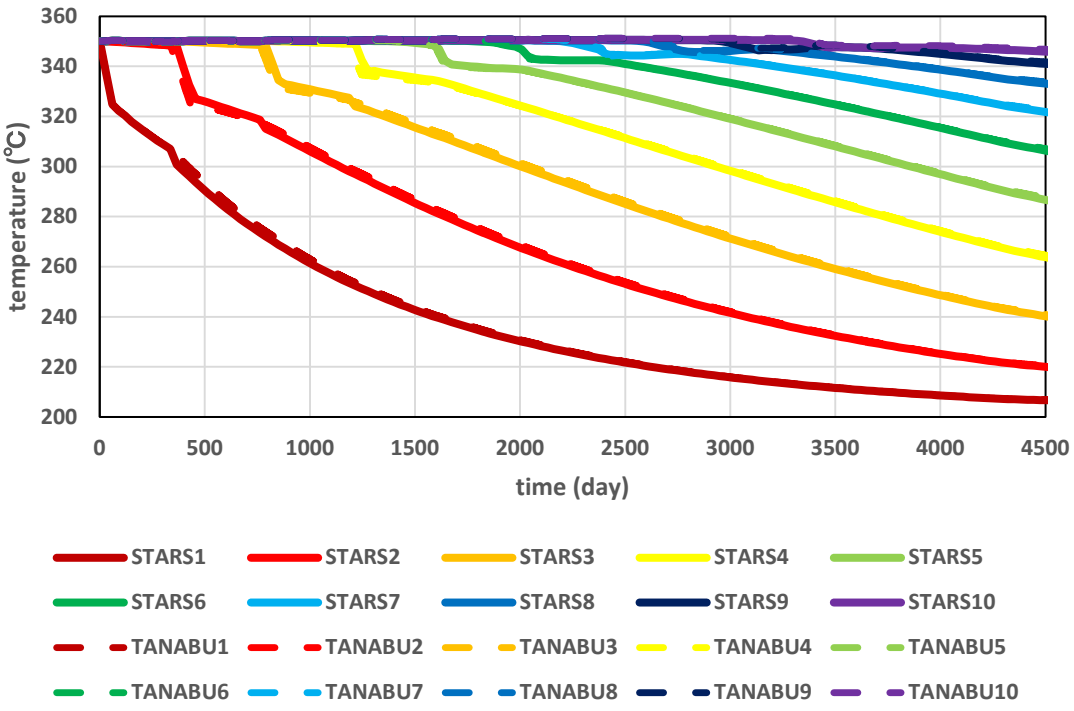

Figure 4: Time vs. temperature

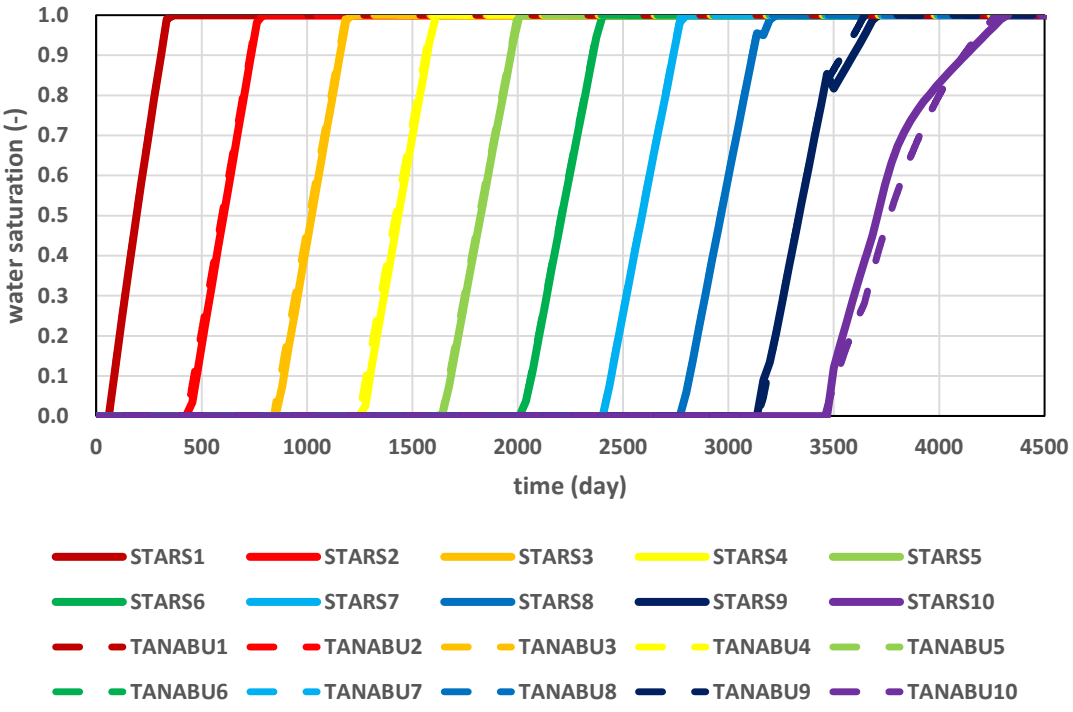

Figure 5: Time vs. water saturation

Since the results by our simulator agree very well with those by STARS, it can be concluded that our simulator works correctly for the cases without chemical reactions.

3.2 Chemical Reaction Calculation Functions

To validate the functions for calculating chemical reactions, we conducted simulation using our simulator and compared the results with the analytical solutions.

3.2.1 Simulation specifications

It was simulated what kind of chemical reactions took place, assuming the initial water phase with various chemical species concentrations as well as the reservoir rock containing calcite ($CaCO_3$), in the closed system (no injection/production) shown in Figure 6. The results of one of such simulations are introduced in this subsection. In this example, the reservoir was assumed to be initially filled with pure water of the temperature of 100 °C. The other properties were the same as those in Subsection 3.1 and the duration of the simulation was 200 days.

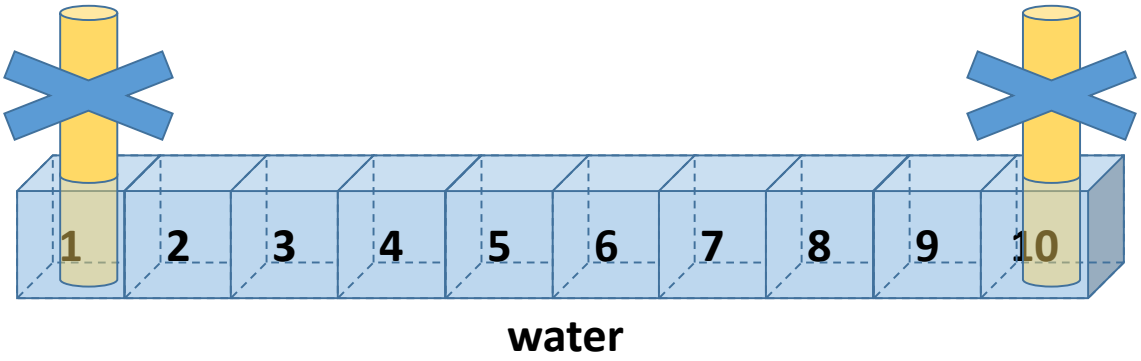

Figure 6: Reservoir model

3.2.2 Results

As shown in Figure 7, the simulated calcium ion concentration in water phase increases and gradually approaches the value of the analytical solution as time passes, reflecting the dissolution of calcite into water phase. It was also confirmed that the concentrations of the other ions approached the analytical solutions as well and that the chemical characteristics such as elevation of boiling point were also changing as suggested by the analytical solutions. From these results, it can be said that the functions for calculating chemical reactions are operating accurately.

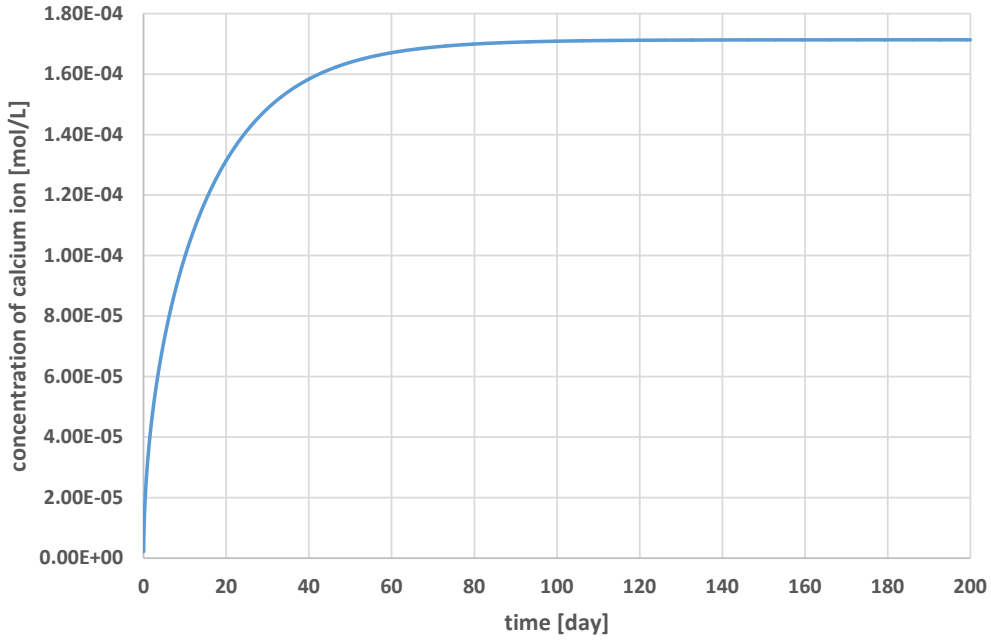

Figure 7: Time vs. concentration of calcium ion

4. Case Studies

We conducted the case studies for evaluating the effects of composition and temperature of injected fluid on reservoir behavior, assuming the following four cases of injection fluids.

Case1: Formation water of the initial reservoir temperature

Case2: Pure water of the initial reservoir temperature

Case3: Supersaturated water of the initial reservoir temperature

Case4: Formation water of the temperature lower than the initial reservoir temperature

4.1 Simulation Specifications

In these case studies, the reservoir was assumed to be initially filled with water (formation water) of the temperature of 200 °C that contained the chemical species in equilibrium with rock mineral of calcite. The other properties were the same as those in Subsection 3.1 as shown in Figure 8 and the duration of simulation time was 4,000 days.

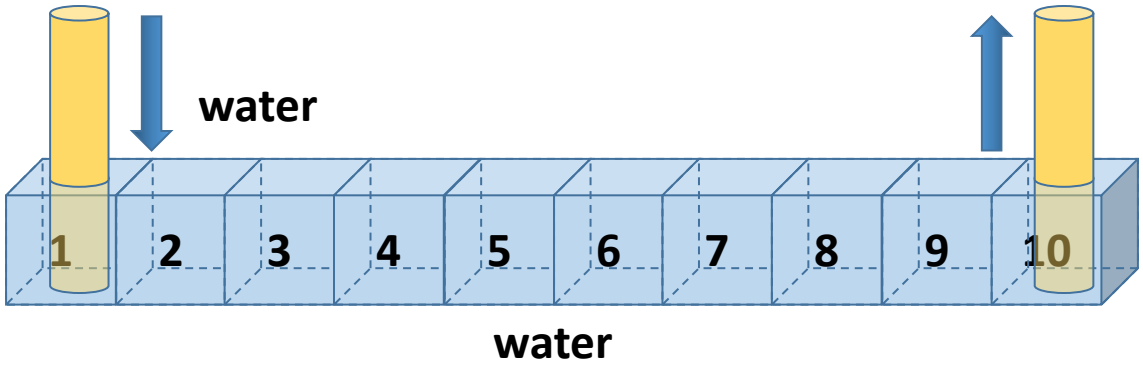

Figure 8: Reservoir model

4.2 Results

The predicted changes in the amount of calcium carbonate and porosity are shown in Figures 9 through 16.

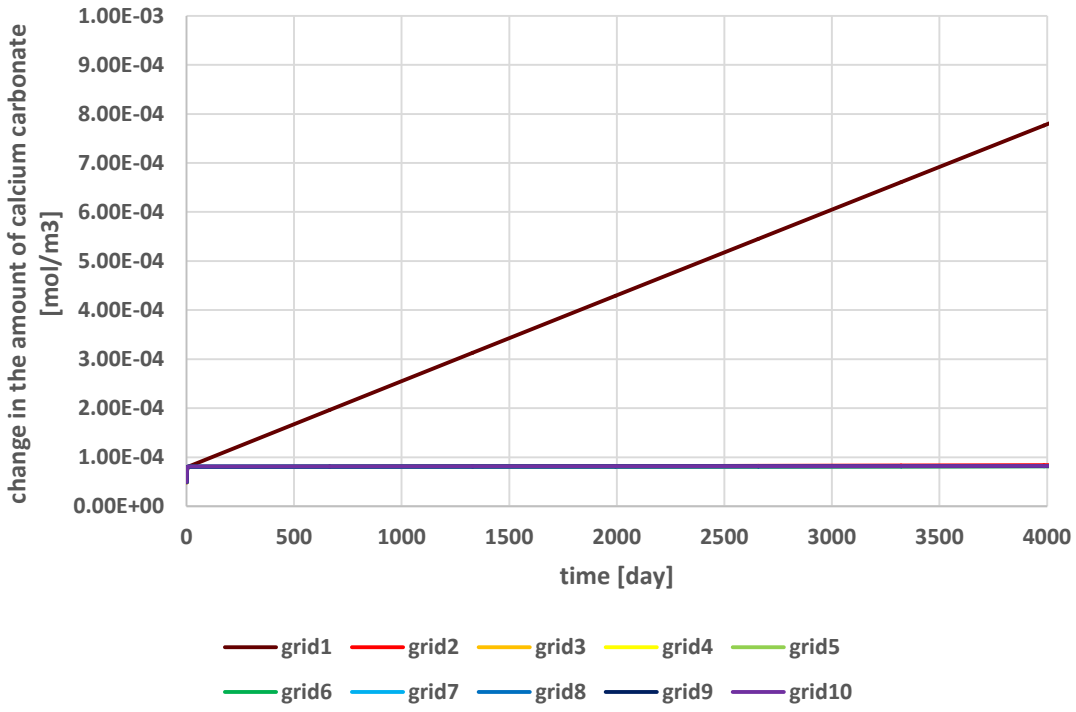

Figure 9: Time vs. changes in amount of calcium carbonate in Case1

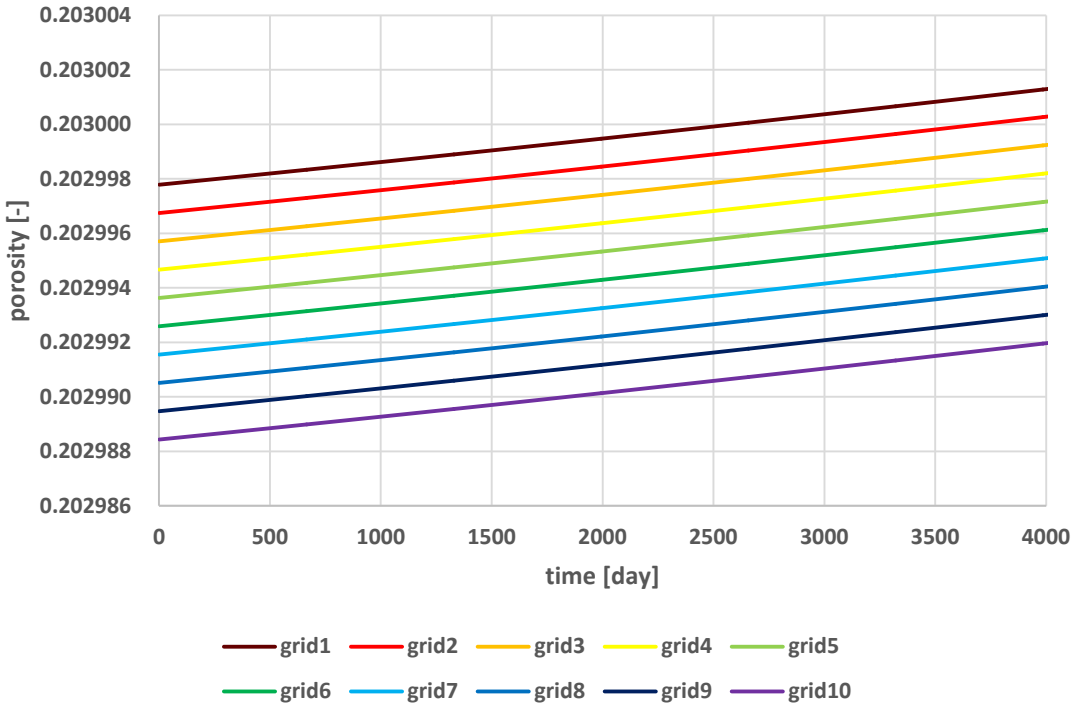

Figure 10: Time vs. porosity in Case1

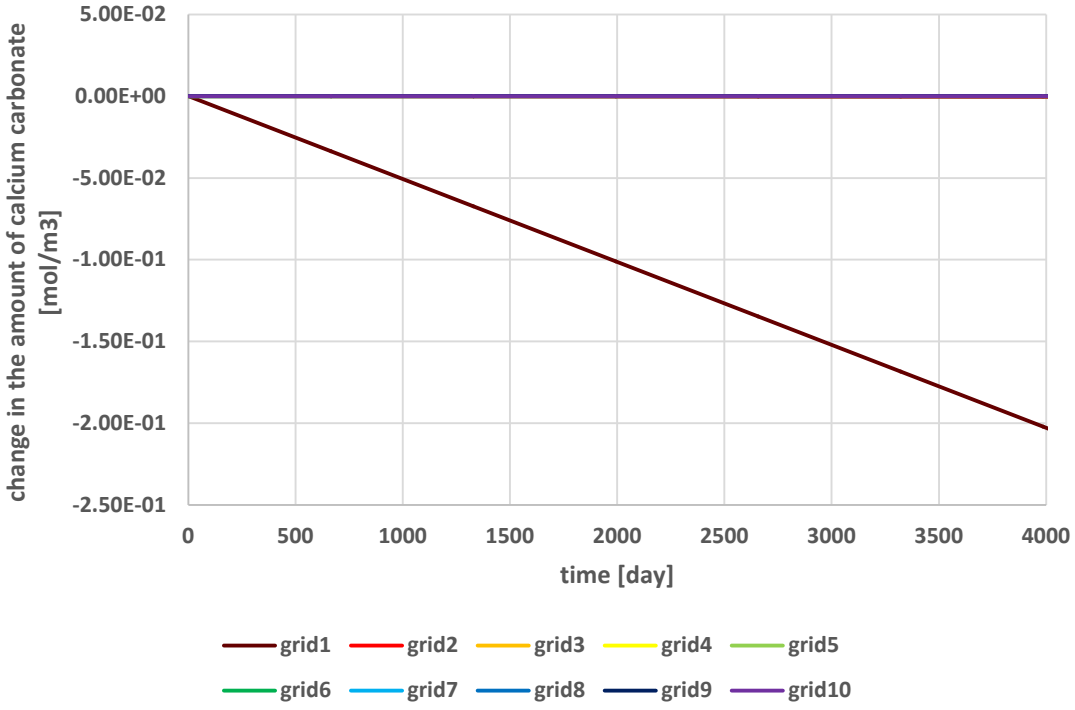

Figure 11: Time vs. changes in amount of calcium carbonate in Case2

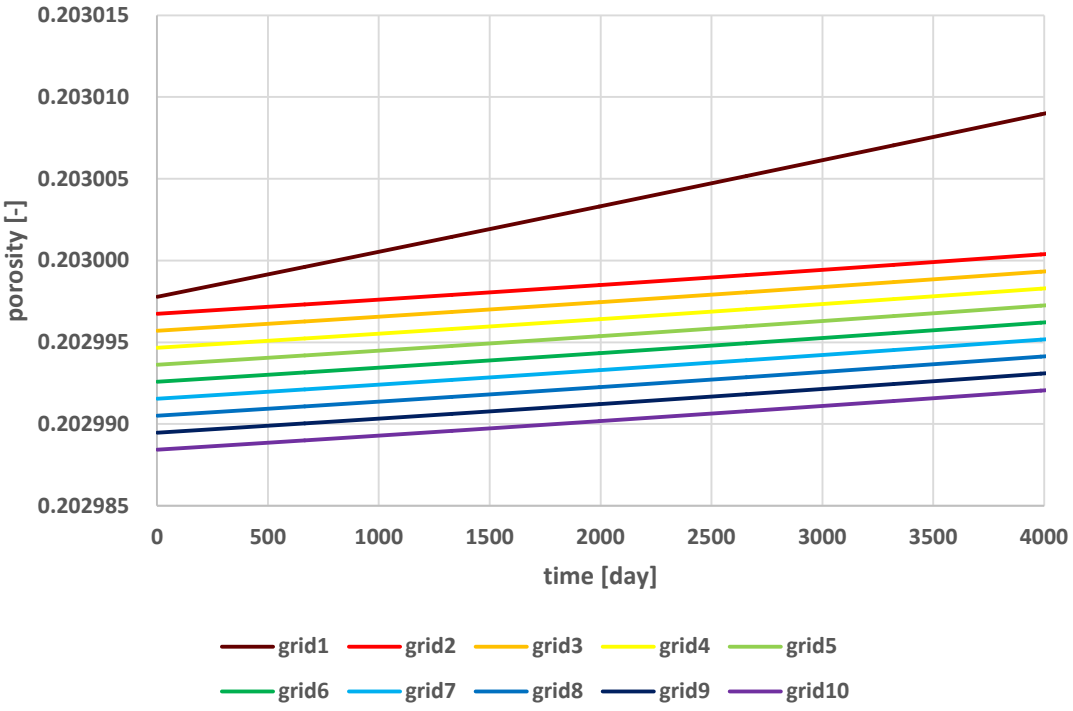

Figure 12: Time vs. porosity in Case2

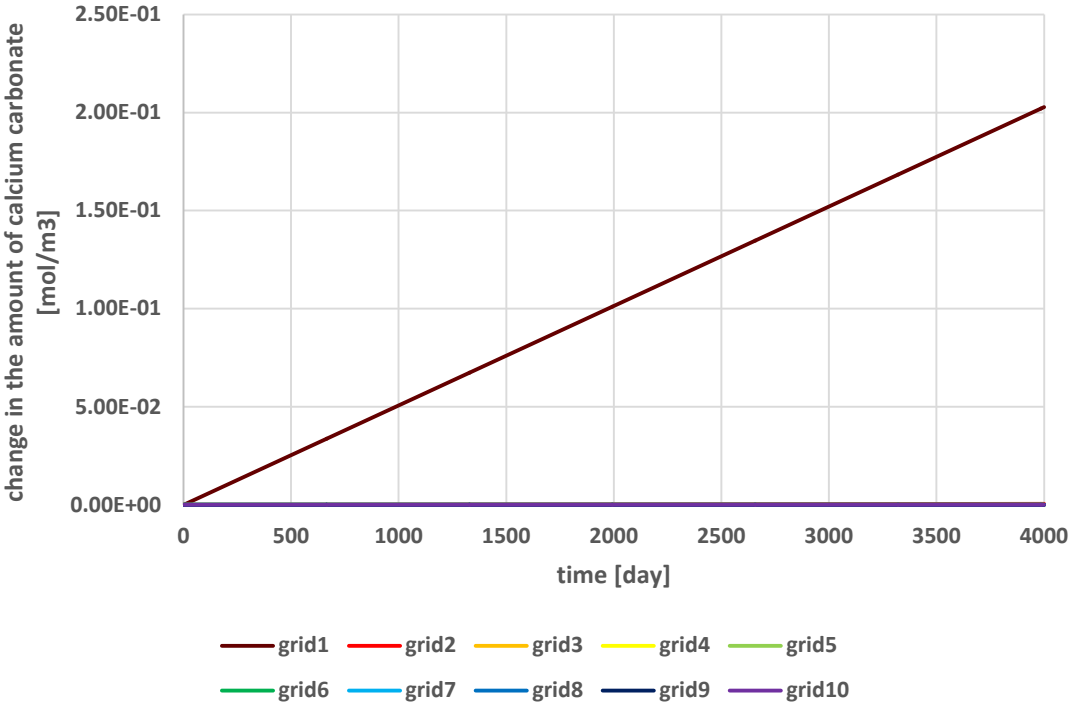

Figure 13: Time vs. changes in amount of calcium carbonate in Case3

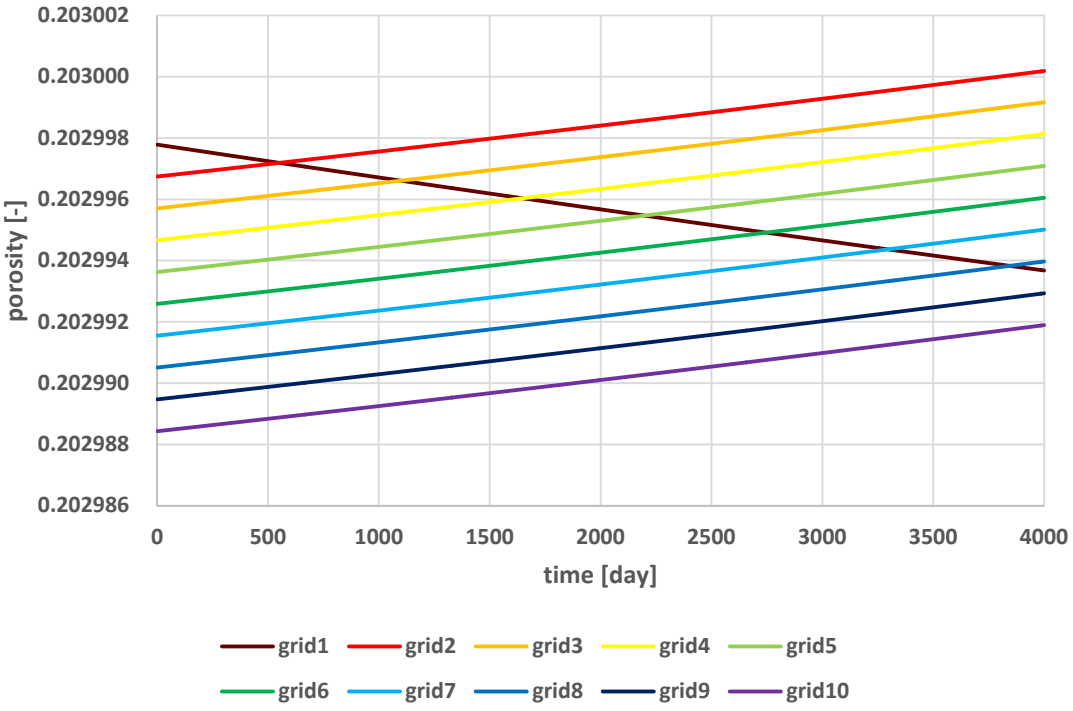

Figure 14: Time vs. porosity in Case3

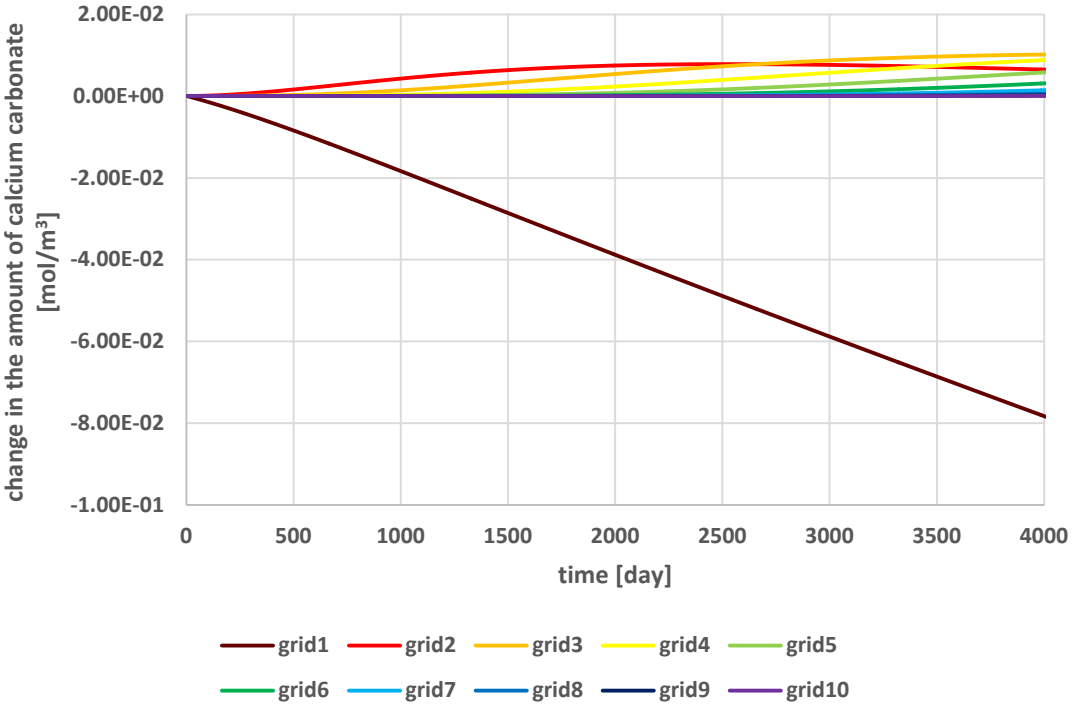

Figure 15: Time vs. changes in amount of calcium carbonate in Case4

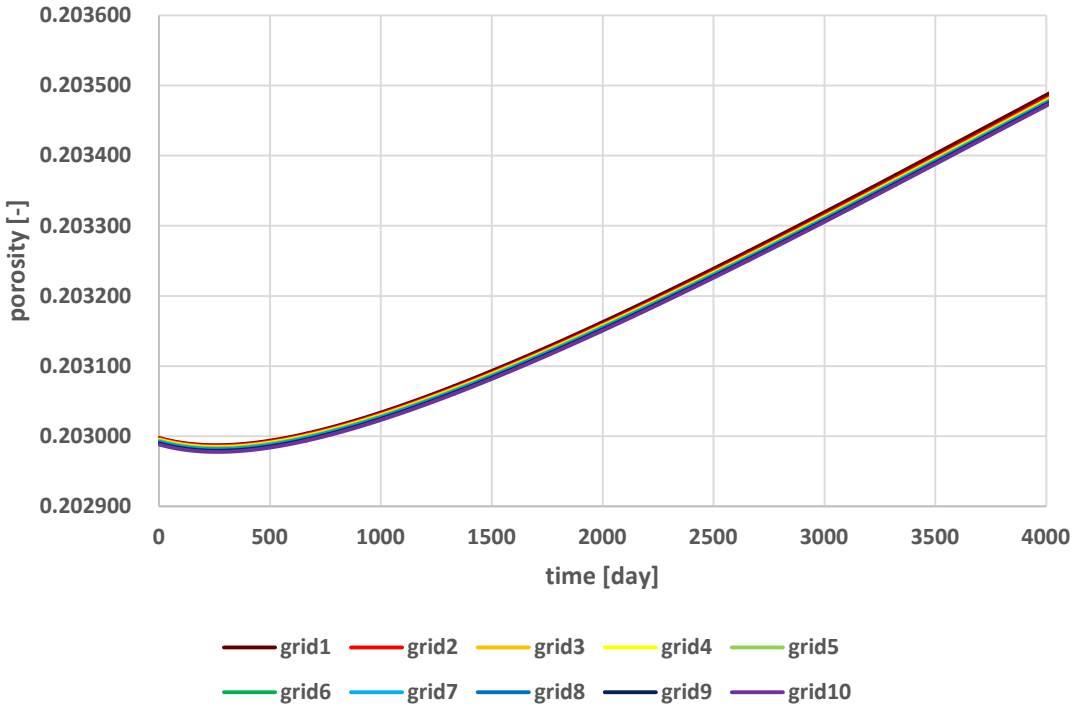

Figure 16: Time vs. porosity in Case4

4.3 Discussion

The following discussion is made on the above simulation results.

4.3.1 Reservoir Behavior in Case1

The changes in the amount of calcium carbonate in Case1 are negligibly small compared with those in the other cases and are within the range of computational errors, suggesting the chemical equilibrium condition throughout the simulation period. The change in porosity is caused not by the dissolution/precipitation of calcium carbonate but by the increasing reservoir pressure.

4.3.2 Comparison between Case1 and Case2

In Case2, since the pure water is injected into the reservoir, the dissolution of calcium carbonate occurs in the grid near the injection well. Along with this, the porosity of grid 1 increases more significantly than that of the other grids.

4.3.3 Comparison of Case1 between Case3

In Case3, contrary to Case2, since the salt concentration of the injection water is high, precipitation of calcium carbonate occurs near the injection well. Along with this, the porosity of grid 1 is significantly reduced.

4.3.4 Comparison of Case1 between Case4

In Case4, even though the composition of the injection fluid is identical to that of the formation water, the temperature of the injection fluid is lower than the initial reservoir temperature. This changes the chemical equilibrium conditions and induces chemical reactions such as dissolution and/or precipitation of calcium carbonate. It is true that these chemical reactions cause the changes in porosity, but in this case the influence of the pressure change is more dominant.

5. Conclusions

In this study, a new geothermal reservoir simulator which can deal with chemical reactions including mineral reactions was successfully developed. From the results of the case studies, the following conclusions were obtained.

(1) The injection of the water with low salt concentration induces the dissolution of rock minerals while that of the water with excessive ion concentration resulted in precipitation of solutes near the injection well.

(2) The change in reservoir temperature causes the mineral dissolution/precipitation due to the alteration of chemical equilibrium.

(3) The magnitude of changes in porosity and permeability associated with dissolution/precipitation of minerals may not be large.

REFERENCES

Computer Modelling Group "STARS User Guide version 2014", (2014).

Fujii, S., Ishigami, Y., and Kurihara, M. "Development of Geothermal Reservoir Simulator for Predicting Three-dimensional Water-Steam Flow Behavior Considering Non-equilibrium State and Kazemi/MINC Double Porosity System" *Geothermal Resources Council Transactions*, 42, (2018), 1762-1798.